Biochimica et Biophysica Acta 1838 (2014) 2243–2249

Contents lists available at ScienceDirect

Biochimica et Biophysica Acta

journal homepage: www.elsevier.com/locate/bbamem

Absorption and folding of melittin onto lipid bilayer membranes via unbiased atomic detail microsecond molecular dynamics simulation ☆

Charles H. Chen [a], Gregory Wiedman [a], Ayesha Khan [b], Martin B. Ulmschneider [a,*]

[a] Department of Materials Science and Engineering, Johns Hopkins University, Baltimore MD, USA
[b] Wolfson Centre for Age Related Disorders, Kings College London, London, UK

ARTICLE INFO

Article history:
Received 24 December 2013
Received in revised form 31 March 2014
Accepted 15 April 2014
Available online 21 April 2014

Keywords:
Melittin
Bilayer
Membrane
Molecular dynamics
Protein folding
Circular dichroism

ABSTRACT

Unbiased molecular simulation is a powerful tool to study the atomic details driving functional structural changes or folding pathways of highly fluid systems, which present great challenges experimentally. Here we apply unbiased long-timescale molecular dynamics simulation to study the *ab initio* folding and partitioning of melittin, a template amphiphilic membrane active peptide. The simulations reveal that the peptide binds strongly to the lipid bilayer in an unstructured configuration. Interfacial folding results in a localized bilayer deformation. Akin to purely hydrophobic transmembrane segments the surface bound native helical conformer is highly resistant against thermal denaturation. Circular dichroism spectroscopy experiments confirm the strong binding and thermostability of the peptide. The study highlights the utility of molecular dynamics simulations for studying transient mechanisms in fluid lipid bilayer systems. This article is part of a Special Issue entitled: Interfacially Active Peptides and Proteins. Guest Editors: William C. Wimley and Kalina Hristova.

1. Introduction

Melittin is a toxic water soluble peptide that is the active compound in honey-bee (*Apis mellifera*) venom. The molecular mechanism is believed to involve transient pore formation in lipid bilayers, which kills target cells by short-circuiting their electrochemical gradient. Experiments have shown that melittin interacts strongly with lipid bilayers, with the monomeric free energy of binding to lipid vesicles in the range of −(5–6) kcal/mol [1,2]. This large gain in free energy is surprising, since melittin is highly soluble in water and its amphiphilic sequence is not indicative of a membrane spanning segment. Circular dichroism experiments have determined that melittin is unstructured in aqueous solution, but forms helical peptides in the presence of lipid vesicles. Oriented circular dichroism experiments show that the tilt angle of bilayer bound melittin is perpendicular to the membrane normal, suggesting that melittin forms helical peptides at the membrane surface [3]. This is consistent with X-ray diffraction experiments of melittin-containing dioleoyl-phosphatidylcholine (DOPC) lipid films that have been deposited on quartz slides, which show that melittin does not penetrate the hydrophobic core of the membrane, but instead resides in the membrane interface at the height of the glycerol-carbonyl groups [3]. Based on all the available evidence, the molecular mechanism of toxicity is currently thought to be: 1. membrane binding and helix formation, 2. interfacial aggregation, and 3. transient pore formation [4–7].

Melittin has been the subject of a number of previous molecular dynamics studies, which have concentrated chiefly on equilibrium structural properties and hydrogen-bonding interactions of individual melittin peptides in various aqueous and organic solvents [8–10], or lipid bilayer membranes [11–13]. Typical simulation lengths of earlier studies are <20 ns and melittin was studied both embedded as a membrane spanning helix [11,12], or on as a surface bound helix [13]. Other simulations have investigated the stability and channel properties of putative pore structures involving bundles of several melittin peptides both in bilayers [14,15] and aqueous environments [16]. More recent works have used umbrella sampling techniques to study the interfacial binding and transmembrane absorption by pulling a single peptide toward a membrane interface and subsequently reorienting them to a transmembrane configuration [17].

While recent multi-microsecond molecular dynamics simulations have explored the configurational equilibrium of helical melittin conformers embedded onto the interface of a palmitoyloleoyl-phosphocholine (POPC) lipid bilayer the atomic detail mechanism of peptide absorption and folding onto the lipid bilayer remains unknown [18].

Here we study this mechanism using unbiased atomic-detail molecular dynamics simulations. The simulations reveal the folding pathway and correctly identify the native state of the peptide on the bilayer surface. Peptide helicity, orientation, and insertion depth are in good agreement with previous experimental and computational measurements.

☆ This article is part of a Special Issue entitled: Interfacially Active Peptides and Proteins. Guest Editors: William C. Wimley and Kalina Hristova.

* Corresponding author.
E-mail address: martin@ulmschneider.com (M.B. Ulmschneider).

http://dx.doi.org/10.1016/j.bbamem.2014.04.012
0005-2736/

2. Results and discussion

2.1. Folding pathway

Melittin absorption and folding onto the membrane were studied via unbiased multi-microsecond atomic detail molecular dynamics simulation. The utility of this *in silico* approach for visualizing the folding-partitioning pathway of peptides in the presence of a lipid bilayer has recently been demonstrated for a number of hydrophobic membrane spanning peptides [19–20]. Initially, a single melittin peptide is placed in bulk water, with the center of mass ~15 Å from the surface of a palmitoyloleoyl-phosphocholine (POPC) lipid bilayer, in a completely extended configuration. The peptide is then allowed to fold freely, as well as partition spontaneously into and out of the lipid bilayer over 2 μs. No restraints or biasing potentials are applied. To increase sampling the temperature of the system was elevated to 120 °C, exploiting the fact that the liquid-to-vapor phase transition can be suppressed in a simulation.

Fig. 1 visually summarizes the folding-partitioning trajectory of the peptide. Melittin rapidly absorbs to the POPC interface ($t_{absorb} < 25$ ns) in an unstructured configuration. Initial contact with the membrane is driven by hydrogen bonds between cationic arginine and lysine residues and the anionic phosphate oxygen atoms of the POPC lipid head groups (Figs. 1 & 2). Helical folding of polypeptide segments is conditional on their burial below the phosphate head groups, while segments that venture out of the bilayer remain unfolded or rapidly unfold again. Folding progresses from the termini, with the central proline residue resisting helix formation for ~1.2 μs. This allows the peptide to sample deeply buried configurations, with proline buried close to the center of the membrane, while the peptide termini remain at the membrane surface (see Fig. 1). Once fully folded the peptide remains remarkably flexible, exploring a large number of strongly bent and kinked configurations with occasional deeply inserted states. A full characterization of the structural and configurational ensemble present at equilibrium typically requires many microseconds, which remains currently unfeasible except on advanced hardware [18]. Similar to folding-partitioning simulations of purely hydrophobic transmembrane segments the non-equilibrium folding process is much shorter than for globular peptides of similar size. This is due to the chemical environment of the membrane, which introduces strong penalties for breaking helical hydrogen-bonds, thus driving rapid secondary structure formation [21,22].

2.2. Folding mechanisms and equilibrium configuration

Unbiased molecular dynamics simulations reveal the atomic details of interfacial folding. Fig. 2 shows that hydrogen bonding contacts between protein and water are only partially replaced by protein–protein and protein–bilayer contacts upon adsorption onto the bilayer interface. Intra-protein hydrogen bonding drives helix formation, which increases to a stable 77 ± 7% after around 1.5 μs (see Fig. 2). This value is a little lower than previous long-timescale simulations of melittin. Starting with surface-absorbed helical conformers these simulations found average peptide helicities in the range of 78–89% [18]. Circular dichroism experiments typically report helicities close to 70% for melittin [1,23–25], but other methods, including amide-exchange measurements, yield average helicities as high as 85% [23,24]. Peptide helicity is not uniform along the sequence. Instead, there are two regions of very high helicity (residues 2–11 and 16–20) separated by a central proline at residue 14. The highly polar C-terminus of the peptide also remains largely unfolded (see Fig. 2).

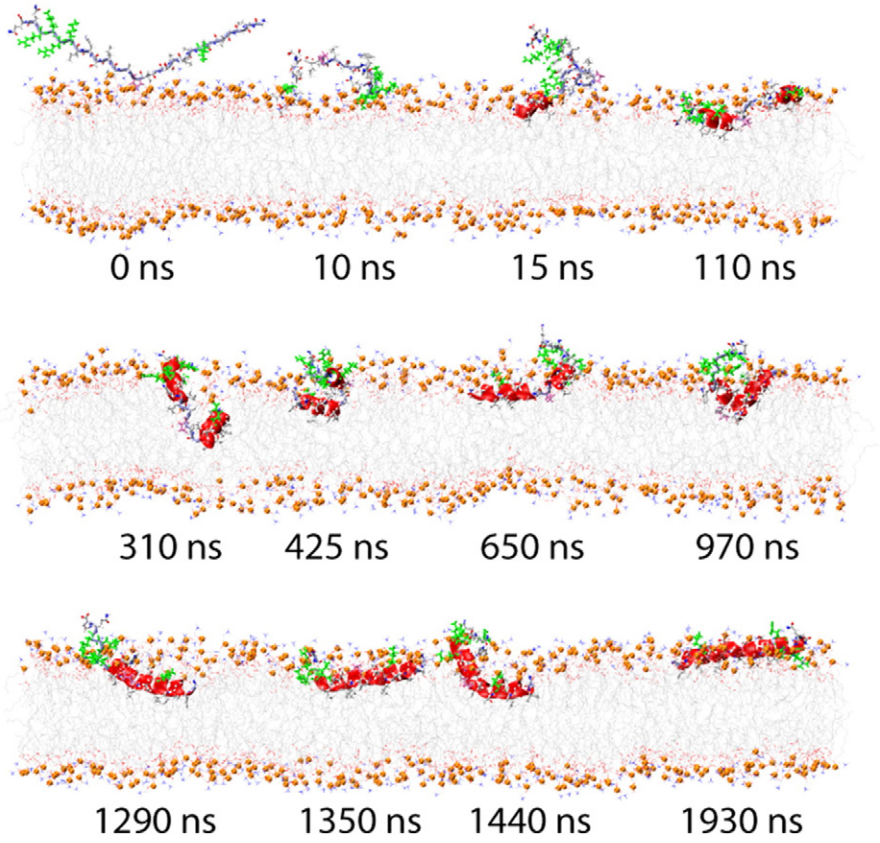

Fig. 1. Interfacial absorption and folding of melittin onto a POPC lipid bilayer. Charged arginine and lysine residues are highlighted in green and the central proline residue is highlighted in mauve. Melittin absorbs rapidly to the bilayer surface. Interfacial folding takes ~1.2 μs to reach the fully folded state, largely due to the central proline residue, which resists helical folding, and allows the peptide to sample deeply buried configurations (e.g. 310 ns & 970 ns). The conformational flexibility of the peptide at the interface is remarkable, with many strongly bent and kinked conformations.

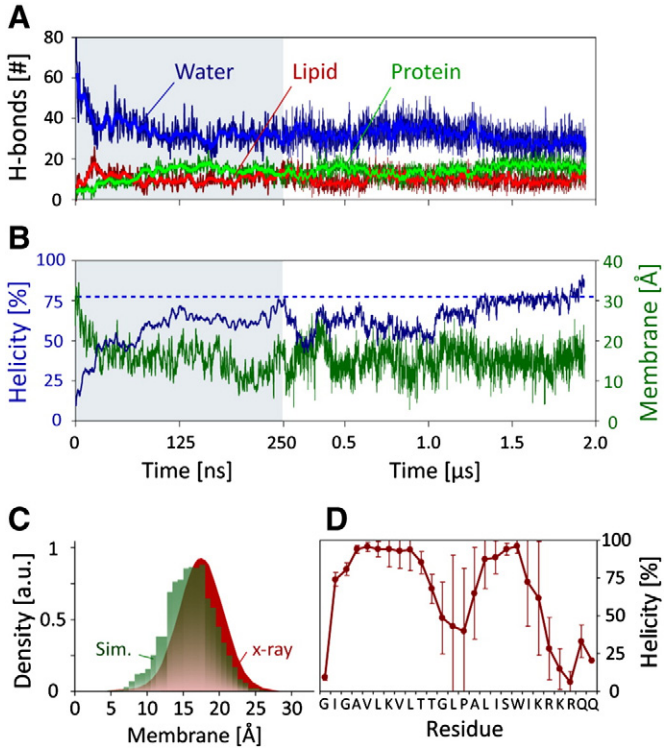

Fig. 2. Melittin absorption and folding. A: Hydrogen bonding contacts between melittin and water (blue), lipid (red), and the peptide itself (green). The figure shows that the loss of hydrating hydrogen bonds is only partially compensated by intra-protein and protein–lipid contacts. Peptide absorption to the interface is visible as an initial spike in the number of protein–lipid contacts at ~20 ns. B: Peptide helicity and elevation above the membrane. Full folding of melittin takes ~1.5 μs. The position on the bilayer surface remains virtually completely bound. C: Histogram of the insertion depth of melittin, collected over the second microsecond of the simulation (green). The previously determined experimental x-ray scattering density in DOPC bilayers is shown for reference (red) [3]. D: Simulation-average of the helicity along the peptide sequence shows two regions of high helicity separated by a central proline residue. The charged C-terminus remains largely unfolded throughout the simulation.

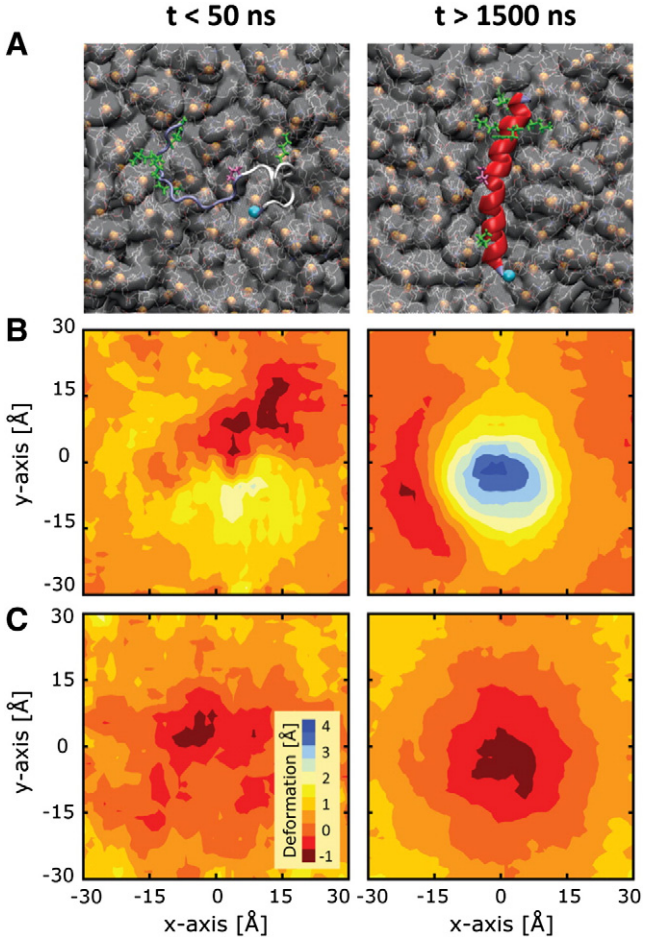

Fig. 3. Melittin-binding induced lipid bilayer deformation. A: Snapshots of melittin at the membrane surface during absorption (t < 50 ns) and after folding at the bilayer surface (t > 1500 ns). B: Bilayer deformation of the leaflet containing the peptide. The figure visualizes the averaged phosphate distance from the bilayer center. C: The melittin induced membrane deformation is clearly visible on the opposite bilayer leaflet.

Fig. 2 shows that the peptide settles close to the glycerol–carbonyl linker at an average distance of 17.3 Å from the center of the bilayer, in excellent agreement with the 17.5 ± 0.3 Å found by X-ray diffraction studies of melittin in planar DOPC bilayers [3], which have a virtually identical hydrophobic core width as POPC.

2.3. Bilayer response

Membranes are two-dimensional fluids that adapt to peptides via deformation. Fig. 3 captures the response of the membrane to the peptide after binding by plotting the spatially and time-averaged deviation of the lipid phosphate groups from their average distance with respect to the center of the bilayer. Initially the membrane deformations are random with only minor undulations that deviate no more than ±2 Å from the average phosphate positions of an unperturbed bilayer. Although experimental and computational trans-bilayer density profiles of membranes containing melittin look largely unperturbed [3,18], binding and folding of melittin nevertheless result in a significant localized deformation, which is lost during the cross-sectional averaging. Folded melittin creates a 4 Å surface bulge that is mirrored as a 1 Å well on the other side of the bilayer (see Supp Fig. 2). Unlike the membrane-interfacial states of purely hydrophobic peptides such as WALP or polyleucine [19,25], melittin is not buried by lipid headgroups arching over and occluding the interfacial helix from the solvent. Instead, the solvent-facing side remains fully accessible over the entire length of the peptide, including the hydrophobic regions (see Fig. 2).

2.4. Melittin thermostability and bilayer binding free energy

The partitioning simulation was carried out at elevated temperature of 120 °C in order to speed up the kinetics of protein folding at the chemically complex bilayer interface. This corresponds to a system in a superheated liquid state, which exploits the fact that the pressure and temperature regulation algorithms of MD simulations cannot simulate the liquid-to-vapor phase transition of the NPT ensemble. We have previously demonstrated the utility of this approach for *ab initio* structure prediction of purely hydrophobic membrane spanning segments, which were experimentally confirmed to be remarkably stable against thermal denaturation [19,25,26]. In order to check the validity of this approach for melittin, a model amphiphilic surface bound peptide, the ability of melittin to resist thermal denaturing in the presence of POPC lipid bilayers was determined experimentally.

Circular dichroism spectra of melittin bound to POPC large unilamellar vesicles (LUVs) show strong helical spectra (see Fig. 4). Heating from 20 to 95 °C results in no change of the spectral profile, suggesting that when absorbed to lipid bilayer membranes these peptides remain helically folded and cannot be denatured easily. Analysis of the peptide ellipticity at 222 nm, which is directly proportional to the helicity of the sample, confirms the absence of a melting transition (see Fig. 4).

These results seem surprising, as experimental and theoretical work by White and co-workers suggests only modest free energy penalties of ~0.5 kcal/mol for breaking an inter-residue peptide hydrogen bond at

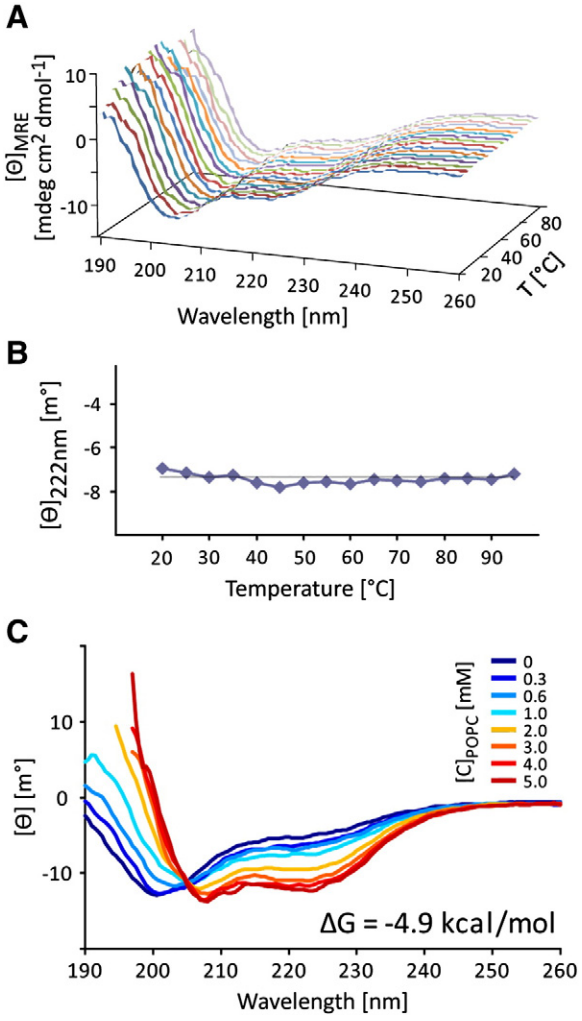

Fig. 4. Experimental determination of melittin binding free energy and thermostability via circular dichroism spectroscopy. A: CD spectra of melittin embedded in POPC LUVs remain helical with no major change discernable up to temperatures of 95 °C, the experimental limit for unpressurized cuvettes. B: Temperature variation of the 222 nm line, which is proportional to the peptide helicity, shows no melting transition, suggestion that any change in the spectra of panel A are due to thermal fraying at the peptide termini or increased noise. C: Vesicle titration of melittin with POPC LUVs at 20 °C, showing the transition from completely unstructured (0 mM POPC) to predominantly helical conformers at 5 mM POPC. The isodichroic point at 205 nm is indicative of a two-state system consisting of unstructured peptides in solution and helical peptide bound to the vesicular membrane surface. Fitting the ellipticity at 222 nm to a thermodynamic model gives a water-to-bilayer binding free energy $\Delta G_{W \rightarrow S} = -4.9$ kcal/mol.

the membrane interface, determined from beta-sheet forming hexapeptides, which indeed denature at ~45 °C [27]. Nevertheless, taking into account the helical surface bound nature of melittin, which buries between a quarter and half of the inter-residue hydrogen bonds close to the hydrophobic membrane core, where the penalty for breaking the peptide bond is ~5 kcal/mol [21], suggests an overall stabilization of 1.6–2.7 kcal/mol per peptide bond. This corresponds to 2–5 kT at room temperature, suggesting that a helical peptide at the membrane interface will resist denaturation up to at least 250 °C, consistent with the present simulation and experimental results.

The ability of hydrophobic membrane spanning polypeptide segments to resist thermal denaturing has been observed previously, with no melting observed for a number of hydrophobic transmembrane segments up to temperatures of 95 °C [19,25], which is the experimental limit for non-pressurized cuvettes. The present results for melittin suggest that interfacial helical peptides are equally stable, for similar energetic reasons.

Once contact between melittin and the lipid head groups on the bilayer surface is established melittin absorbs rapidly and does not unbind again, which suggests strong binding, but precludes determination of the absorption free energy. Direct quantification of the peptide partitioning free energy requires measurable populations of water-solvated and membrane bound peptides. In order to determine the binding free energy experimentally we measured the change in peptide helicity upon titration with lipid vesicles. Fig. 4 shows the change in the circular dichroism (CD) spectra of 35 μM melittin upon titration with thermodynamically stable LUVs. The spectra show that the peptide changes from an unstructured configuration in water to a helix in the presence of POPC LUVs. An isodichroic point at 205 nm is indicative of an equilibrium of two states: 1. unstructured melittin in water, and 2. helical melittin bound to the POPC LUVs. Fitting the change in mean residue ellipticity at 222 nm to a thermodynamic model allows estimation of the binding free energy to POPC lipid bilayers (see Methods for details) [28], which was found to be -4.9 ± 0.1 kcal/mol at 20 °C, similar to previous measurements, which found a partitioning free energy of −6.0 kcal/mol [1]. It should be noted that at peptide to lipid ratios of 1/30 and 1/100 peptide aggregation upon binding cannot be excluded.

Interestingly, the estimated apparent free energy of translocon mediated partitioning (ΔG_{app}) of melittin is −5.2 kcal/mol [29], which is very similar to the actual interfacial partitioning free energy obtained here (-4.9 ± 0.1 kcal/mol) and in previous spectroscopic measurements (see Supp. Fig. 1). The total hydrophobic moment is 5.7.

2.5. Initial configuration and temperature dependence

Configurational ensembles (i.e. the structures and locations of the peptide) at equilibrium are independent of the starting configuration of a simulation. However, in the absence of high resolution experimental data it is difficult to determine if a simulation has reached and fully sampled equilibrium. Ideally, a large number of equilibrium simulations with different starting conditions should be performed, and each simulation should be sampled until they all converge onto the same configurational ensemble. However, the computational cost associated with such an approach is prohibitive. In the case of melittin, the equilibrium structural ensemble is known from circular dichroism experiments, providing a reference point to determine if a long simulation has reached equilibrium. In order to decrease the computational cost of the simulation the unfolded peptide was initially placed in close proximity to the membrane surface thus making the system as small as possible. In addition the temperature was elevated to 120 °C to prevent kinetic trapping of folding intermediates. The implicit assumption is that the native state has a very low free energy and is thus not significantly perturbed by heating. Given the experimentally determined stability against thermal denaturing and the strong free energy of folding-partitioning these assumptions seem reasonable (Fig. 4).

In order to check that heating to 120 °C does not perturb the folding-partitioning pathway a repeat simulation was performed at 90 °C (Fig. 5 & Table 1). At this temperature the results can be directly compared to the experimental circular dichroism measurements. The peptide follows the same overall pathway of rapid unfolded partitioning and slow interfacial folding. As expected, both the partitioning and folding kinetics are significantly slower at 90 °C and melittin requires >0.5 μs to reach >50% helicity, compared to 25 ns at 120 °C. Although melittin does not reach stable native helicity over the ~2 μs timeframe of the simulation interfacial folding is similar and characterized by a continuous build up of peptide helicity. As in the 120 °C simulation the central proline residue resists helix formation and presents the key barrier to complete folding. Nevertheless, the result suggests that if continued the peptide will eventually fold to full native helicity. This is consistent with circular dichroism experiments (Fig. 4), which showed no significant spectral change for melittin embedded into POPC upon heating to 90 °C. As in the simulation the peptide remains fully helical, suggesting no major structural changes in the equilibrium ensemble.

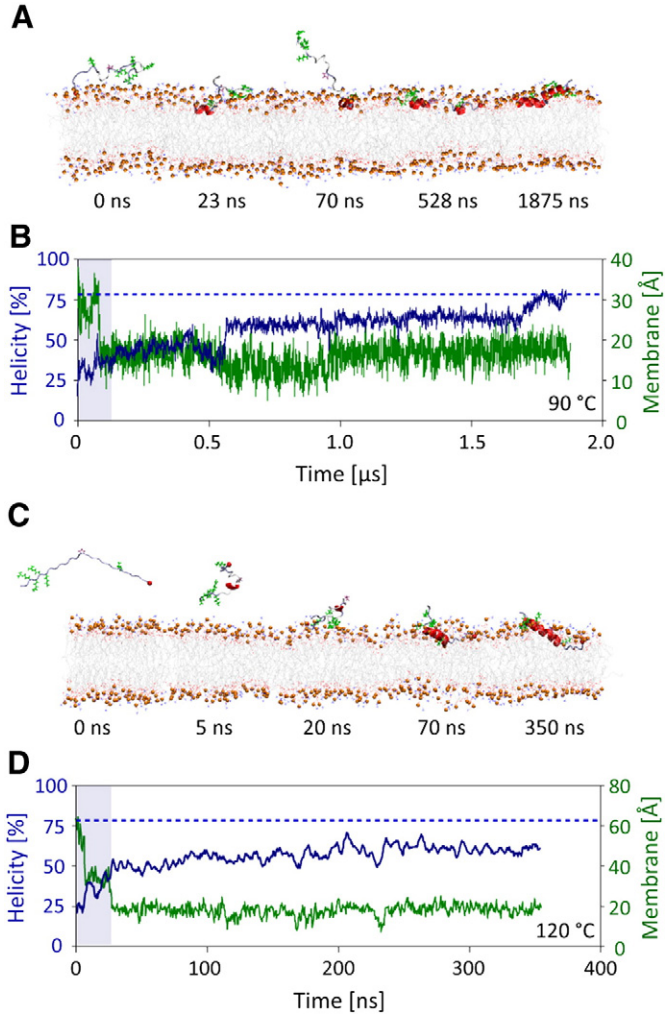

Fig. 5. Control simulations. A: Partitioning-folding simulation at 90 °C. The system is identical to that described in Figs. 1 & 2. B: The peptide absorbs unfolded to the interface and does not reach native helicity during the 1.9 μs timeframe of the simulation. C & D: A repeat simulation with the peptide further from the bilayer surface shows similar absorption, folding, and partitioning behavior than described in Figs. 1 & 2. For both systems absorption is rapid (shaded) and followed by slow interfacial folding.

In order to check that the initial positioning of the peptide in close proximity to the membrane does not bias the non-equilibrium folding-partitioning pathway a set of four simulations was performed with the peptide center of mass spaced >30 Å away from the bilayer surface (see Table 1). At this distance the closest atoms are ~20 Å from the membrane surface, which is larger than the non-bonded interaction cut-off. These simulations are much more costly, as the number of atoms is almost double that of the smaller system described above. Fig. 5 shows that at 120 °C the partitioning-folding pathway is virtually identical to the smaller system, although the 350 ns timeframe of the simulation is too short to capture full folding. Repeat simulation of the same system at 20, 50, and 80 °C show that lowering the temperature slows down peptide precipitation onto the bilayer surface, presumably due to reduced translational sampling (see Supp. Fig. 3). In summary, the data suggest that neither the choice of initial positioning of the peptide, nor the elevation of the simulation temperature above 100 °C has a major effect on the partitioning-folding pathway, or the native state equilibrium of the peptide.

Table 1
Summary of the simulations. †All systems contain 100 mM sodium chloride. ‡t_{Absorb}, $t_{Half\text{-}fold}$, and t_{Fold} are the times for absorption (peptide hydrogen-bonding with lipids), folding to >50% helicity (half-folded melittin), and >80% helicity (fully folded melittin) respectively. As folding is stochastic and a half-folded melittin might unfold completely before refolding these times are only indicative of the speed of secondary structure formation on the interface, rather than actual folding-timescales. Similarly, melittin must retain its helicity for at least 50 ns above 50 and 80% to be assumed half-folded and folded respectively.

Name	System† [Peptide/lipids/water]	Length [ns]	T [°C]	N_{trans} [#]	$t^{‡}_{Absorb}$ [ns]	$t^{‡}_{Half\text{-}fold}$ [ns]	$t^{‡}_{Fold}$ [ns]
Mel1	1/98/3577	2000	120	1	13	25	1331
Mel2	1/98/3577	1900	90	1	81	563	–
Mel3	1/98/6394	50	20	1	–	–	–
Mel4	1/98/6394	50	50	1	–	–	–
Mel5	1/98/6394	50	80	1	20	–	–
Mel6	1/98/6394	350	120	1	27	30	–

3. Conclusion

Unbiased long-timescale molecular simulations were used to explore the atomic details of membrane absorption and interfacial folding of melittin, a template for pore-forming amphiphilic membrane active peptides. The peptide was found to bind strongly to the lipid bilayer in an unstructured configuration and rapidly folds into a predominantly helical configuration with the helix long-axis oriented perpendicular to the membrane normal at the height of the lipid glycerol–carbonyl linker. Melittin forms a localized surface deformation in the bilayer and remains solvent accessible along the entire length of the helix. The simulations revealed that the surface bound native helical conformer is highly resistant against thermal denaturation, and the results are confirmed by circular dichroism spectroscopy experiments. This study highlights the utility of molecular dynamics simulations for studying transient mechanisms in fluid lipid bilayer systems.

4. Methods

4.1. Modeling and simulations

Completely extended melittin (sequence: GIGAVLKVLTTGLPALISW IKRKRQQ) was placed in bulk water with the center of mass 15 Å from the surface of a pre-equilibrated 98 POPC lipid bilayer. The system was equilibrated for 10 ns with strong restraints on the peptide backbone to hold the extended structure in place above the membrane. For the production run all restraints were removed and no biasing potentials of any type were used in the simulations.

Molecular dynamics simulations were performed and analyzed with gromacs 4.5 (www.gromacs.org) [30] and hippo beta (www.biowerkzeug.com), using the CHARMM27 all-atom protein force field [31], in conjunction with the TIP3P water model [32]. CHARMM36 all-atom lipid parameters for POPC were taken from Klauda et al. [33]. Electrostatic interactions were computed using PME, and a cutoff of 10 Å was used for van der Waals interactions. Bonds involving hydrogen atoms were constrained using LINCS [34]. The integration time-step was 2 fs and neighbor lists were updated every 5 steps. All simulations were performed in the NPT ensemble, without any restraints or biasing potentials. Water, lipids, and the protein were each coupled separately to a heat bath with time constant $\tau_T = 0.1$ ps using velocity rescale temperature coupling [35]. Atmospheric pressure of 1 bar was maintained using weak semi-isotropic pressure coupling with compressibility $\kappa_z = \kappa_{xy} = 4.6 \cdot 10^{-5}$ bar^{-1} and time constant $\tau_P = 1$ ps [36].

4.2. Sample preparation

Peptides were solid phase synthesized using Fmoc/HBTU chemistry, purified using reverse phase high pressure liquid chromatography (HPLC), and quantified using mass spectroscopy as described previously [37,38]. Melittin was solvated in 10 mM phosphate buffer and peptide concentration was determined using tryptophan absorption at 280 nm, assuming an average molar extinction coefficient of $\varepsilon = 5600$ M^{-1} cm^{-1} [39].

Palmitoyloleoyl-phosphocholine (POPC) lipids were purchased from Avanti Polar Lipids (Alabaster, AL, USA). Large unilamellar vesicles (LUVs) in 10 mM phosphate buffer (pH 7.0) were obtained via extrusion through 100 nm membranes. Samples were prepared by mixing peptide and LUV solutions.

4.3. Binding free energy

Peptide binding to POPC bilayers was determined via vesicle titration. Melittin solutions (35 μM) in 10 mM phosphate buffer (pH 7.0) were titrated with 3 μL aliquots of 100 mM POPC LUVs in identical buffer. Circular dichroism (CD) spectra were recorded using a JASCO J-810 spectra-polarimeter, and at the ANKA and Bejing synchrotron radiation CD beamlines. Spectra were recorded from 260 to 190 nm with a stepsize of $\Delta\lambda = 0.5$ nm, bandwidth $= 0.5$ nm, and a dwell time of 2 s. Each spectrum was averaged over 6–12 repeat scans. The averaged spectra were normalized to molar ellipticity per residue.

4.4. Thermostability assay

A circular dichroism temperature scan was performed via CD spectroscopy using a similar setup as for the binding free energy. Samples of melittin bound to POPC LUVs were measured in a 1 mm cuvette with 10–35 μM peptide and 1.0 mM lipid concentrations corresponding to a peptide to lipid ratio of ~1/30–1/100. Temperature was controlled with a Peltier device, and varied between 20 and 95 °C in 5° steps. The sample was equilibrated for 5 min at each temperature before collecting data, and measurements were repeated 5 times.

4.5. Analysis

Peptide helicity is calculated for each residue and averaged over the complete sequence. A residue is considered helical if its backbone dihedral angles are within $\pm 40°$ from the ideal α-helical values ($\Phi = -57°$, $\Psi = -47°$).

Error bars are estimated by dividing the simulations into a series of 10 blocks of equal length, and performing averaging for each block. The error bars are given by $\pm\sigma$, where σ is the standard deviation of the mean, i.e. the standard deviation of the individual block averages with respect to the overall average.

The total hydrophobic moment of amino acid sequences and apparent partitioning free energy (ΔG_{app}) of the peptide between water and membrane were estimated using MPEx (http://blanco.biomol.uci.edu/mpex/), a software tool developed by Stephen White at UCI [20].

Acknowledgements

The authors would like to thank Kalina Hristova for helpful discussions and providing experimental equipment and materials. G.W. was supported by a NSF DMR grant (# 1003441). Circular dichroism beamtime at the ANKA (Karlsruhe Institute of Technology, Germany) and Beijing (National Academy of Sciences, Beijing, China) synchrotron radiation facilities is gratefully acknowledged.

Appendix A. Supplementary data

Supplementary data to this article can be found online at http://dx.doi.org/10.1016/j.bbamem.2014.04.012.

References

[1] A.S. Ladokhin, M. Fernandez-Vidal, S.H. White, CD spectroscopy of peptides and proteins bound to large unilamellar vesicles, J. Membr. Biol. 236 (2010) 247–253.
[2] H. Vogel, Incorporation of melittin into phosphatidylcholine bilayers. Study of binding and conformational changes, FEBS Lett. 134 (1981) 37–42.
[3] K. Hristova, C.E. Dempsey, S.H. White, Structure, location, and lipid perturbations of melittin at the membrane interface, Biophys. J. 80 (2001) 801–811.
[4] L. Yang, T.A. Harroun, T.M. Weiss, L. Ding, H.W. Huang, Barrel-stave model or toroidal model? A case study on melittin pores, Biophys. J. 81 (2001) 1475–1485.
[5] H. Raghuraman, A. Chattopadhyay, Melittin: a membrane-active peptide with diverse functions, Biosci. Rep. 27 (2007) 189–223.
[6] P.F. Almeida, A. Pokorny, Mechanisms of antimicrobial, cytolytic, and cell-penetrating peptides: from kinetics to thermodynamics, Biochemistry 48 (2009) 8083–8093.
[7] G. van den Bogaart, J.V. Guzman, J.T. Mika, B. Poolman, On the mechanism of pore formation by melittin, J. Biol. Chem. 283 (2008) 33854–33857.
[8] R.B. Sessions, C.E. Gibbs, C.E. Dempsey, Hydrogen bonding in helical polypeptides from molecular dynamics simulations and amide hydrogen exchange analysis: alamethicin and melittin in methanol, Biophys. J. 74 (1998) 138–152.
[9] D. Roccatano, M. Fioroni, M. Zacharias, G. Colombo, Effect of hexafluoroisopropanol alcohol on the structure of melittin: a molecular dynamics simulation study, Protein Sci. 14 (2005) 2582–2589.
[10] D. Roccatano, G. Colombo, M. Fioroni, A.E. Mark, Mechanism by which 2,2,2-trifluoroethanol/water mixtures stabilize secondary-structure formation in peptides: a molecular dynamics study, Proc. Natl. Acad. Sci. U. S. A. 99 (2002) 12179–12184.
[11] M. Bachar, O.M. Becker, Protein-induced membrane disorder: a molecular dynamics study of melittin in a dipalmitoylphosphatidylcholine bilayer, Biophys. J. 78 (2000) 1359–1375.
[12] A. Glattli, I. Chandrasekhar, W.F. van Gunsteren, A molecular dynamics study of the bee venom melittin in aqueous solution, in methanol, and inserted in a phospholipid bilayer, Eur. Biophys. J. 35 (2006) 255–267.
[13] S. Bernèche, M. Nina, B. Roux, Molecular dynamics simulation of melittin in a dimyristoylphosphatidylcholine bilayer membrane, Biophys. J. 75 (1998) 1603–1618.
[14] J.-H. Lin, A. Baumgartner, Stability of a melittin pore in a lipid bilayer: a molecular dynamics study, Biophys. J. 78 (2000) 1714–1724.
[15] S.J. Irudayam, M.L. Berkowitz, Influence of the arrangement and secondary structure of melittin peptides on the formation and stability of toroidal pores, Biochim. Biophys. Acta 1808 (2011) 2258–2266.
[16] P. Liu, X. Huang, R. Zhou, B.J. Berne, Observation of a dewetting transition in the collapse of the melittin tetramer, Nature 437 (2005) 159–162.
[17] S.J. Irudayam, M.L. Berkowitz, Binding and reorientation of melittin in a POPC bilayer: computer simulations, Biochim. Biophys. Acta 1808 (2011) 2975–2981.
[18] M. Andersson, J.P. Ulmschneider, M.B. Ulmschneider, S.H. White, Conformational states of melittin at a bilayer interface, Biophys. J. 104 (2013) L12–L14.
[19] J.P. Ulmschneider, J.C. Smith, S.H. White, M.B. Ulmschneider, In silico partitioning and transmembrane insertion of hydrophobic peptides under equilibrium conditions, J. Am. Chem. Soc. 133 (2011) 15487–15495.
[20] M.B. Ulmschneider, J.P.F. Doux, J.A. Killian, J. Smith, J.P. Ulmschneider, Mechanism and kinetics of peptide partitioning into membranes, J. Am. Chem. Soc. 132 (2010) 3452–3460.
[21] S.H. White, W.C. Wimley, Membrane protein folding and stability: physical principles, Annu. Rev. Biophys. Biomol. Struct. 28 (1999) 319–365.
[22] A.S. Ladokhin, S.H. White, Folding of amphipathic α-helices on membranes: energetics of helix formation by melittin, J. Mol. Biol. 285 (1999) 1363–1369.
[23] H. Vogel, F. Jähnig, The structure of melittin in membranes, Biophys. J. 50 (1986) 573–582.
[24] C.E. Dempsey, G.S. Butler, Helical structure and orientation of melittin in dispersed phospholipid membranes from amide exchange analysis in situ, Biochemistry 31 (1992) 11973–11977.
[25] M.B. Ulmschneider, J.P. Doux, J.A. Killian, J.C. Smith, J.P. Ulmschneider, Mechanism and kinetics of peptide partitioning into membranes from all-atom simulations of thermostable peptides, J. Am. Chem. Soc. 132 (2010) 3452–3460.
[26] M.B. Ulmschneider, J.C. Smith, J.P. Ulmschneider, Peptide partitioning properties from direct insertion studies, Biophys. J. 98 (2010) L60–L62.
[27] W.C. Wimley, K. Hristova, A.S. Ladokhin, L. Silvestro, P.H. Axelsen, S.H. White, Folding of beta-sheet membrane proteins: a hydrophobic hexapeptide model, J. Mol. Biol. 277 (1998) 1091–1110.
[28] S.H. White, W.C. Wimley, A.S. Ladokhin, K. Hristova, Protein folding in membranes: determining energetics of peptide-bilayer interactions, Methods Enzymol. 295 (1998) 62–87.
[29] C. Snider, S. Jayasinghe, K. Hristova, S.H. White, MPEx: a tool for exploring membrane proteins, Protein Sci. 18 (2009) 2624–2628.
[30] H.J.C. Berendsen, D. van der Spoel, R. van Drunen, GROMACS: a message-passing parallel molecular dynamics implementation, Comput. Phys. Commun. 95 (1995) 43–56.
[31] A.D. MacKerell, D. Bashford, Bellott, R.L. Dunbrack, J.D. Evanseck, M.J. Field, S. Fischer, J. Gao, H. Guo, S. Ha, D. Joseph-McCarthy, L. Kuchnir, K. Kuczera, F.T.K. Lau, C. Mattos, S. Michnik, T. Ngo, D.T. Nguyen, B. Prodhom, W.E. Reiher, B. Roux, M. Schlenkrich, J. C. Smith, R. Stote, J. Straub, M. Watanabe, J. Wiórkiewicz-Kuczera, D. Yin, M. Karplus, All-atom empirical potential for molecular modeling and dynamics studies of proteins†, J. Phys. Chem. B 102 (1998) 3586–3616.
[32] W.L. Jorgensen, J. Chandrasekhar, J.D. Madura, R.W. Impey, M.L. Klein, Comparison of simple potential functions for simulating liquid water, J. Chem. Phys. 79 (1983) 926–935.
[33] J.B. Klauda, R.M. Venable, J.A. Freites, J.W. O'Connor, D.J. Tobias, C. Mondragon-Ramirez, I. Vorobyov, A.D. MacKerell Jr., R.W. Pastor, Update of the CHARMM all-atom additive force field for lipids: validation on six lipid types, J. Phys. Chem. B 114 (2010) 7830–7843.
[34] B. Hess, H. Bekker, H.J.C. Berendsen, J.G.E.M. Fraaije, LINCS: a linear constraint solver for molecular simulations, J. Comput. Chem. 18 (1997) 1463–1472.

[35] G. Bussi, D. Donadio, M. Parrinello, Canonical sampling through velocity rescaling, J. Chem. Phys. 126 (2007) 014101.
[36] H.J.C. Berendsen, J.P.M. Postma, W.F. Vangunsteren, A. Dinola, J.R. Haak, Molecular-dynamics with coupling to an external bath, J. Chem. Phys. 81 (1984) 3684–3690.
[37] M.R. de Planque, J.A. Kruijtzer, R.M. Liskamp, D. Marsh, D.V. Greathouse, R.E. Koeppe II, B. de Kruijff, J.A. Killian, Different membrane anchoring positions of tryptophan and lysine in synthetic transmembrane alpha-helical peptides, J. Biol. Chem. 274 (1999) 20839–20846.
[38] M.R.R. de Planque, E. Goormaghtigh, D.V. Greathouse, R.E. Koeppe, J.A.W. Kruijtzer, R.M.J. Liskamp, B. de Kruijff, J.A. Killian, Sensitivity of single membrane-spanning alpha-helical peptides to hydrophobic mismatch with a lipid bilayer: effects on backbone structure, orientation, and extent of membrane incorporation, Biochemistry 40 (2001) 5000–5010.
[39] C.N. Pace, F. Vajdos, L. Fee, G. Grimsley, T. Gray, How to measure and predict the molar absorption coefficient of a protein, Protein Sci. 4 (1995) 2411–2423.